International Journal of Computer Applications (0975 - 8887)
Volume 187 - No.78, February 2026

Multi-Disease Detection and Classification using a Lightweight Convolutional Neural Network

Soumya Pal
Department of Computer and System Sciences
Visva-Bharati University
Santiniketan, West Bengal, India

Kakali Datta
Department of Computer and System Sciences
Visva-Bharati University
Santiniketan, West Bengal, India

Debarka Mukhopadhyay
Department of Computer Science and Engineering
Christ University
Bengaluru, India

Paramartha Dutta
Department of Computer and System Sciences
Visva-Bharati University
Santiniketan, West Bengal, India

ABSTRACT

Convolutional Neural Networks (CNNs) have become essential tools in automated medical diagnostics, delivering strong performance across a wide range of medical imaging types. In this study, we introduce a 17-layer CNN—made up of 15 convolutional layers and 2 fully connected layers—designed to detect and classify brain tumors, COVID-19, pneumonia, and breast cancer from multimodal images, including MRI scans, chest X-rays, and histopathological slides.

The model is first trained on balanced datasets to develop stable and generalizable feature representations, and then fine-tuned on real-world, imbalanced data using a weighted random sampling technique to account for class distribution differences. Cross-validation results show high accuracy across all tasks: 99.97% for brain tumor detection, 99.96% for COVID-19, 98.06% for pneumonia, and 94.87% for breast histopathology.

To boost generalization and reduce overfitting, the architecture incorporates batch normalization, transfer learning, and strategic data resampling. Diagnostic performance is further validated using ROC curves, precision–recall metrics, and confusion matrices. By effectively addressing common challenges like class imbalance and domain variability, this work demonstrates the real-world potential of deep learning models to enhance clinical decision-making and support precision medicine.

General Terms

Medical Imaging, Deep Learning, Diagnostic Systems

Keywords

Convolutional Neural Network (CNN), Brain Tumor Detection, COVID-19 Diagnosis, Breast Histopathology, Pneumonia Identification, Multimodal Medical Imaging

1. INTRODUCTION

The landscape of medical diagnostics is rapidly evolving, fueled by the growing adoption of deep learning and its integration with multimodal medical imaging. Early and precise identification of diseases such as brain tumors, COVID-19, breast cancer (via histopathological analysis), and pneumonia is critical to improving clinical outcomes, enabling timely interventions, and advancing the goals of precision medicine. However, despite recent advancements, deep learning-based diagnostic systems continue to face several limitations that hinder their widespread clinical adoption.

One of the foremost challenges lies in maintaining diagnostic consistency across different imaging modalities. MRI scans, histopathological slides, and chest X-rays differ significantly in structure, resolution, and data distribution, making it difficult for a single model to perform reliably across them. Additionally, real-world medical datasets are often imbalanced—conditions like rare tumor types are underrepresented—which can bias the learning process and weaken the model's ability to generalize, especially for minority classes. Variability in image quality and acquisition settings, particularly in chest X-rays and COVID-19 scans, further introduces noise that undermines prediction stability. Many high-performing models also require significant computational resources, making them unsuitable for deployment in low-power environments or real-time clinical applications. Moreover, most existing approaches are narrowly focused on single diseases or imaging types, lacking the flexibility needed for broader diagnostic use.

To address these challenges, this study proposes a compact and efficient 15-layer Convolutional Neural Network (CNN) designed to support multi-disease detection across diverse imaging sources. Proposed model is optimized not only for high diagnostic accuracy but also for generalization and deployment efficiency. The key contributions of this work are as follows:

This work introduces a two-stage training approach, where the model is first pretrained on balanced datasets to learn robust fea-

tures, and then fine-tuned on real-world imbalanced datasets using transfer learning to improve adaptability.
Weighted random sampling and targeted data augmentation techniques to enhance learning from underrepresented classes and reduce overfitting.
A unified CNN architecture is developed to integrate MRI, histopathology, and chest X-rays, allowing for accurate multi-disease classification within a single framework.
The model achieves high test accuracy across all tasks: 99.97% for brain tumor detection, 99.96% for COVID-19, 94.57% for breast histopathology, and 98.06% for pneumonia.
The proposed model is lightweight and computationally efficient, making it suitable for real-time diagnostic environments such as telemedicine and AI-assisted clinical workflows. The framework addresses key challenges in multimodal medical image analysis, including data integration, class imbalance, and generalization, while demonstrating consistent performance across multiple disease categories and imaging modalities.
The remainder of the paper is organized as follows. Section 2 reviews related work. Sections 3, 4, and 5 describe the datasets, model architecture, and methodology, respectively. Section 6 presents experimental results, including loss and accuracy curves, precision–recall and ROC analyses, confusion matrices, and comparative evaluations, along with an ablation study on the Brain Tumor dataset. Section 7 presents the appendices, and Section 8 concludes the paper.

2. RELATED WORK

Nyoman Abiwinanda et al.[2] developed a CNN to spontaneously classify the three most frequent types of Brain Tumors(BTR), namely Glioma, Meningioma, and Pituitary, without the need for region-based pre-processing requests. They used a BTR dataset of 3064 T-1 weighted CE-MRI of the brain to train the CNN, freely accessible on Figshare Cheng (Brain Tumor Dataset, 2017 [6]). At best, they attained a training accuracy of 98.51 % and a validation accuracy of 84.19 %.
P. Afshar et al. [3] have used capsules rather than neurons to develop deep learning architecture and to overcome the deficiencies of the requirement of a large amount of training data in the CNN. Capsule networks are vigorous to rotation and affine modification and require significantly less training data, as is the case when processing clinical picture datasets such as brain MRI scans. They have achieved 82.30% prediction accuracy.
Seetha J et al. [16] proposed an automated BTR detection model using CNN classification.
Gulshan et al. [12] proposed a model that can automatically detect brain tumors from MRI images and classify them into two categories, i.e., tumor and non-tumor. They have used the "Leaky ReLU" activation function, i.e. (Conv2D + Leaky ReLU) layers combination. They have achieved 78.57 % accuracy for the unseen data.
In 2021, Tingting Liu et al.[13] proposed an automated brain tumor diagnosis system. Four main elements comprise the method: preprocessing, segmentation, feature extraction, and final categorization. Discrete Wavelet Transform (DWT) and Gray Level Cooccurrence Matrix (GLCM) extract characteristic features of MRIs, which are forwarded to an optimized CNN diagnosis. This method uses the Sparrow Search Algorithm (ESSA) classification to optimize CNN. This proposed algorithm performed the best with an accuracy of 94.77%.
A genetic algorithm-based edge detection technique was introduced by AHMED H et al.[1] in 2020. The authors detect the fine edges using the proposed method, which is applied to the appropriate training dataset with the implemented GA edge detection algorithm. The proposed method yielded an average accuracy of 99.09%.
B Kalyan et al. [Kalyan and Reddy 2022] use three models, Resnet50, VGG19, and DenseNet121, and compare their accuracy on a dataset of 253 MRI scan data items, and also RMProp optimizer is used to compile the models. This optimizer implements gradient descent, allowing authors to adjust the weights of the model in an optimized way to improve the accuracy.
Using deep neural network (DNN) architectures, Amin et al.[5] proposed a new architecture for detecting brain tumors. The model uses three convolutional layers, three rectified linear units (ReLU), and a softmax layer for classification. The proposed model took an average of 5.502 seconds to run.
The modern imaging technique of contrast-enhanced 3D gradient echo (CE 3D GRE) has been proposed by Jun et al.[10] to detect brain metastases by suppressing blood vessels. Patients were selected randomly to train and test (39 sets).
In 2014, Komal Sharma, Akwinder Kaur, and Shruti Gujral [18] proposed a study to develop a machine learning-based brain tumor detection system. The Multilayer Perceptron and Naïve Bayes machine learning algorithms are used for classification.
In 2017, S. S. Hunnur, A. Raut, and S. Kulkarni [9] demonstrated brain tumor detection using thresholding algorithms and described the comparative study about tumor detection. The obtained results are shown, demonstrating efficient tumor detection and tumor boundary extraction using the Sobel edge detection operator.
In [8], a completely automated brain tumor classification method is proposed based on DNN.
In [14] the author proposed a scheme for brain tumor detection using the CNN technique. The system uses this suggested technique to provide an MRI image in JPEG format. The system then detects the brain tumor in the image. The authors use the augmentation technique to create a large dataset. Thus, they get more samples of the same MRI image with different angles by augmentation to produce accurate results.
In [7] Sreeparna Das, Ishan Ayus, and Deepak Gupta wire a review on COVID-19. In this paper [17], the DAG3Net model was trained in which the X-ray images were standardized within a specific size and dimensions to make the classification levels equal between the two categories (COVID-19 and Non-Covid-19) and to meet the requirements of the classification model.
In [4], the study proposed a CNN model that takes a 2D chest X-ray image input with the size of 224×224×3 called "COV-X".This model includes four convolutional layers and four max-pooling layers; one max-pooling layer follows each convolution layer. Dropout layers were added after max pooling and dense layers to avoid overfitting. In 2021, Swapnil Singh [19] intends to develop a method for automating the detection of pneumonia using chest X-rays and comparing convolutional neural networks and multilevel perceptron.In this paper [15], a Convolution Neural Network was designed from square one, unlike in other papers where researchers have used transfer learning to achieve a good score comparable to transfer learning techniques.
Naresh Khuriwal and Nidhi Mishra [11] are applying deep learning technology to the MIAS Database and have a 98% accuracy on breast cancer.
Fabio Alexandre Spanhol, Luiz S. Oliveira, Caroline Petitjean, and Laurent Heutte [20] propose a method based on extracting image patches for training the CNN and the combination of these patches for final classification. This method allows high-resolution histopathological images from BreaKHis as input to existing CNN,

avoiding model adaptations that can lead to a more complex and computationally costly architecture.
The table below presents a comprehensive evaluation of diverse methodologies, dataset utilization, performance metrics, and limitations. It illuminates the distinctive strategies employed in each study, shedding light on their strengths and challenges in advancing the field of medical image classification.

3. DATASETS

The effectiveness and generalization ability of medical image classification models are heavily influenced by the quality, size, and diversity of the datasets used during training. For this study, The study focuses on four disease categories: brain tumors, COVID-19, breast cancer (via histopathological analysis), and pneumonia. All datasets were sourced from publicly available repositories on Kaggle. For each disease, two versions of the dataset were used—one balanced and one imbalanced—to simulate both controlled and real-world data scenarios.
Each dataset included binary class labels. The brain tumor dataset was labeled as Tumor and No Tumor, while the COVID-19 dataset comprised COVID and Normal classes. For breast histopathology, images were categorized into IDC Positive (1) and IDC Negative (0). The pneumonia dataset included Pneumonia and Normal classes.
The balanced datasets were used for initial training to allow the model to learn stable and unbiased features. These included:
7,010 brain tumor images (approximately 3,500 per class),
800 COVID-19 chest X-rays (around 400 per class),
135,000 breast histopathology images (roughly 67,500 per class),
10,730 pneumonia X-rays (about 5,365 per class).
To simulate real-world clinical conditions, imbalanced datasets were also used:
253 brain tumor images (155 Tumor, 98 No Tumor),
94 COVID-19 images (69 COVID, 25 Normal),
2,212 breast histopathology samples (833 IDC Positive, 1,379 IDC Negative),
5,856 pneumonia images (4,273 Pneumonia, 1,583 Normal).
Each imbalanced dataset was split into training, validation, and test sets using a 70:15:15 ratio. The training set was used to fit the model's parameters, the validation set helped tune hyperparameters and monitor performance during training, and the test set, which remained unseen throughout the training process, was used for final evaluation to measure how well the model generalized to new, unseen data.
This dual-dataset approach—starting with balanced data and transitioning to imbalanced, real-world distributions—allowed the model to learn robust features while still being tested under realistic diagnostic conditions.

4. MODEL ARCHITECTURE

4.1 Proposed Model

This study introduces a 17-layer Convolutional Neural Network (CNN) architecture designed for the classification of brain tumors, COVID-19, breast histopathology, and pneumonia, as illustrated in Fig. 1. The network comprises 15 convolutional layers and 2 fully connected layers. Batch normalization follows each convolutional layer to improve stability and convergence, and max-pooling layers provide Fig.1: The Proposed Model spatial down sampling. The model achieves test accuracies of 99.97 percent for brain tumor detection, 99.96 percent for COVID-19, 94.57 percent for breast histopathology, and 98.06 percent for pneumonia.

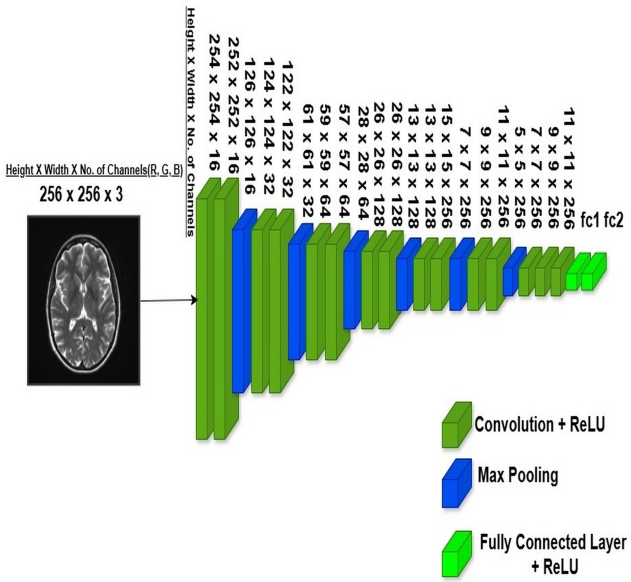

Fig. 1: The Proposed Convolutional Neural Network Model.

4.2 Layer Configuration

The CNN developed in this study is designed to be both efficient and effective across various medical imaging tasks. It consists of five sequential convolutional blocks followed by a fully connected classification section. The network gradually increases in depth and complexity, enabling it to learn both low-level and high-level features. Here's a detailed breakdown:
Convolutional Block 1 This initial block contains two convolutional layers, each with 16 filters and a 3×3 kernel. Both layers use a stride of 1 and no padding. A 2×2 max-pooling layer follows, reducing the spatial dimensions of the feature maps while retaining important information.
Convolutional Block 2 The second block also includes two convolutional layers but increases the number of filters to 32. These layers use the same 3×3 kernel and stride of 1, without padding. Another 2×2 max-pooling operation is applied afterward to further downsample the output.
Convolutional Block 3 This block follows the same structure, with two convolutional layers using 64 filters. The pooling operation remains consistent—2×2 max-pooling—to manage the feature map size as depth increases.
Convolutional Block 4 The fourth block expands to three convolutional layers, all using 128 filters. The first layer applies no padding, while the next two use padding of 1 to preserve spatial resolution. A max-pooling layer with a 2×2 window is again used to reduce dimensionality.
Convolutional Block 5 This is the deepest block in the network and contains six convolutional layers, each with 256 filters and 3×3 kernels. All layers in this block use padding of 2 to widen the receptive field without shrinking the spatial size too quickly.
Normalization and Activation Every convolutional layer is followed by batch normalization to stabilize the learning process and speed up convergence. ReLU (Rectified Linear Unit) activation is applied next to introduce non-linearity, helping the model learn complex patterns.

Flattening After the final convolutional block, the output feature maps are flattened into a one-dimensional vector, making them compatible with the dense layers that follow.
Fully Connected Layers The final stage of the model consists of two fully connected (dense) layers. Each is followed by 1D batch normalization and ReLU activation, which help improve feature representation and reduce the risk of overfitting before the model makes its final prediction.

4.3 Loss and Activation Function:

The model generates raw output scores, or logits, at the final layer, without applying a softmax activation during the forward pass. Instead of explicitly normalizing these outputs, classification is handled using the CrossEntropyLoss() function. This loss function is widely used in multi-class classification tasks as it internally applies the softmax operation to the logits and then computes the cross-entropy between the predicted probabilities and the true class labels. This design keeps the forward pass computationally efficient and ensures numerical stability during training.

5. METHODOLOGY

For each disease category, namely Brain Tumor, COVID-19, Pneumonia, and Breast Histopathology, two types of datasets were constructed: a balanced dataset and an imbalanced dataset. This design enabled a systematic evaluation of model performance under both ideal and real-world class distribution conditions.
To mitigate the effects of class imbalance and reduce the risk of overfitting, data augmentation and resampling techniques were employed. Specifically, imbalanced datasets were trained using a weighted random sampling strategy, which assigns higher sampling probabilities to minority-class samples during the training process. The weighted random sampler selects training samples based on predefined class weights, ensuring that underrepresented classes appear more frequently within each training batch. This approach maintains a more balanced class distribution during training, even when the original dataset is highly skewed. As a result, the model is encouraged to learn discriminative features across all classes and reduces bias toward majority-class samples.
A transfer learning strategy was adopted in the proposed framework. Initially, the convolutional neural network was trained from scratch using the balanced datasets to learn stable and generalizable feature representations. The learned weights from this stage were subsequently transferred to train the model on the imbalanced datasets.
For the imbalanced datasets, the data were partitioned into training, validation, and test sets using a 70:15:15 split. The training set was used for model optimization, the validation set facilitated hyperparameter tuning and performance monitoring, and the test set was kept completely unseen during training to ensure an unbiased final evaluation.
Using this two-stage training strategy, the proposed model achieved test accuracies of 99.97 percent for Brain Tumor classification, 99.96 percent for COVID-19 detection, 94.87 percent for Breast Histopathology analysis, and 98.06 percent for Pneumonia classification.

6. RESULTS AND DISCUSSION

6.1 Experimental Setup

All experiments were conducted using the proposed 17-layer CNN implemented in PyTorch. Training ran on a Linux-based GPU environment with an NVIDIA T4 (8 GB VRAM), supported by an Intel Xeon processor at roughly 2.3 GHz and CUDA-enabled drivers. The T4 operated with a base clock near 585 MHz. The Adam optimizer was used with a learning rate of 1.4×10^{-5}, weight decay of 1×10^{-4}, and a batch size of 16. CrossEntropyLoss was the objective function. The two-stage training process included 30 epochs of pretraining on balanced datasets and 150 epochs of fine-tuning on imbalanced datasets using Weighted Random Sampling. All experiments were repeated with multiple random seeds to ensure stable and reproducible results.

Layer (type)
Conv2d - 1
Conv2d - 2
MaxPool2d - 3
Conv2d - 4
BatchNorm2d - 5
Conv2d - 6
BatchNorm2d - 7
Maxpool2d - 8
Conv2d - 9
BatchNorm2d - 10
Conv2d - 11
BatchNorm2d - 12
MaxPool2d - 13
Conv2d - 14
BatchNorm2d - 15
Conv2d - 16
BatchNorm2d - 17
MaxPool2d - 18
Conv2d - 19
BatchNorm2d - 20
Conv2d - 21
BatchNorm2d - 22
Maxpool2d - 23
Conv2d - 24
BatchNorm2d - 25
Conv2d - 26
BatchNorm2d - 27
MaxPool2d - 28
Conv2d - 29
BatchNorm2d - 30
Conv2d - 31
BatchNorm2d - 32
Conv2d - 33
BatchNorm2d - 34
Flatten - 35
Linear - 36
BatchNorm1d - 37
Linear - 38
Total params: 11,622,034
Trainable params: 11,622,034
Non-Trainable params: 0

6.2 K-Fold Cross Validation

The proposed methodology incorporates a rigorous k-fold cross-validation procedure with k = 10. This approach ensures robustness

and reliability in evaluating the performance of the proposed convolutional neural network across diverse datasets. This process was meticulously applied to the train datasets of each category, entailing five epochs for validation accuracy in each fold and subsequently computing the average validation accuracy.Here, the results in Table 1 are as follows:

Table 1. : K-Fold Cross Validation Table

Datasets	Fold	Average Validation Accuracy
COVID-19[7]	1	1.0000
	2	1.0000
	3	1.0000
	4	1.0000
	5	1.0000
	6	1.0000
	7	1.0000
	8	1.0000
	9	1.0000
	10	1.0000
Brain Tumor[7]	1	1.0000
	2	1.0000
	3	1.0000
	4	1.0000
	5	1.0000
	6	1.0000
	7	1.0000
	8	1.0000
	9	1.0000
	10	1.0000
Breast Histopathology[7]	1	0.9819
	2	0.9745
	3	0.9915
	4	0.9915
	5	0.9926
	6	0.9904
	7	0.9755
	8	0.9713
	9	0.9904
	10	0.9958
Pneumonia[7]	1	0.9904
	2	0.9864
	3	0.9920
	4	0.9928
	5	0.9928
	6	0.9908
	7	0.9944
	8	0.9932
	9	0.9936
	10	0.9956

6.3 Loss Curves

Figures 2 through 5 illustrate the loss curves for brain tumor, COVID-19, breast histopathology, and pneumonia datasets, all processed by the proposed model. In each case, both training and validation losses exhibit rapid convergence, reflecting the model's efficient learning and strong generalization.

Fig. 2 illustrates the brain tumor loss curve, where both training and validation losses converge rapidly, with a sharp decline within the first 30 epochs. The close alignment of these losses suggests a well-balanced model, demonstrating excellent generalization across the training and validation datasets.

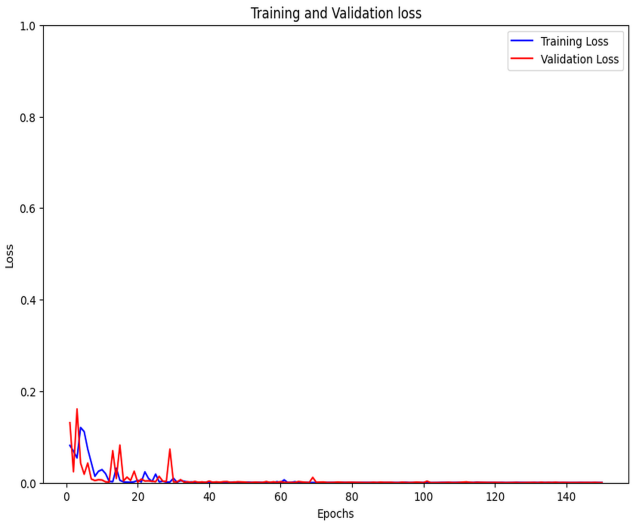

Fig. 2: Loss curve of brain tumor dataset.

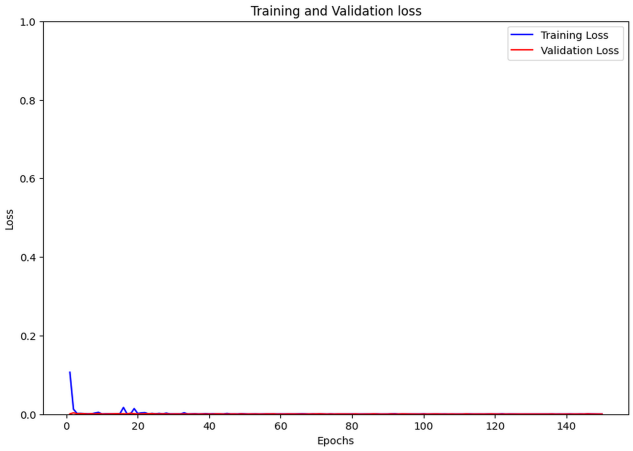

Fig. 3: Loss curve of COVID-19 dataset.

In Fig. 3 the COVID-19 loss curve exhibits an impressive early convergence, with both losses stabilizing at low levels shortly after training begins. This rapid learning process suggests that the model is highly efficient, quickly mastering the complexities of the dataset.

In Fig. 4 the loss curve for the breast histopathology model demonstrates a consistently low training loss, indicating that the model effectively captures the underlying patterns in the data. The variations observed in the validation loss suggest that the model is highly responsive to different data features, highlighting its sensitivity and adaptability.

In Fig. 5 the pneumonia loss curve displays a low and stable training loss, reflecting the model's effectiveness in learning from the data. The model's behavior during validation demonstrates its capacity to adapt to various data conditions, highlighting its flexibility.

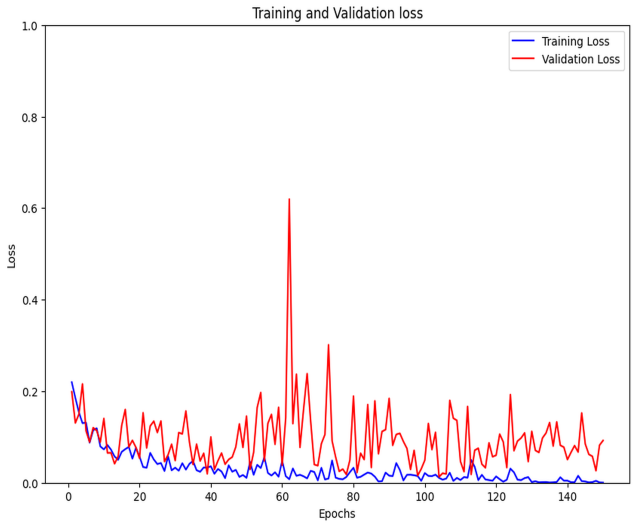

Fig. 4: Loss curve of breast histopathology dataset.

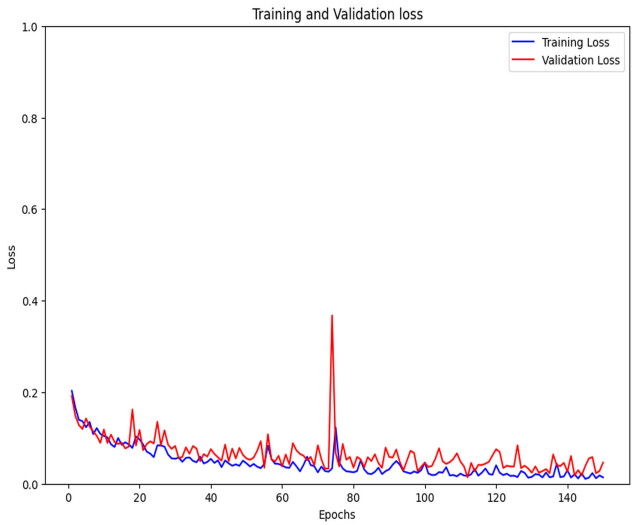

Fig. 5: Loss curve of pneumonia dataset.

6.4 Accuracy Curves

Figures 6 through 9 showcase the accuracy curves for brain tumor, COVID-19, breast histopathology, and pneumonia detection, all derived from the proposed model applied to different datasets.
In Fig. 6 the accuracy curve of brain tumor detection exhibits robust and consistent accuracy, with both training and validation accuracies reaching near-perfect levels early in the training process. This rapid convergence and sustained high accuracy signify the model's effectiveness in identifying brain tumors.
In Fig. 7 the COVID-19 detection accuracy curve the model continues to deliver exceptional results, with both training and validation accuracies converging quickly to 1.0. This demonstrates the model's proficiency in detecting COVID-19 cases with a high degree of precision.

In Fig. 8 The accuracy curve of breast histopathology exhibits exceptional performance with both training and validation accuracies consistently approaching nearly 1.0. This demonstrates the model's strong ability to accurately distinguish and classify IDC (Invasive Ductal Carcinoma) positive and negative images, enhancing the effectiveness of diagnostic differentiation.
In Fig. 9 the accuracy curve for Pneumonia demonstrates the model's exceptional performance on the dataset, with both training and validation accuracies approaching nearly to 1.0. The consistent accuracy across epochs highlights the model's robustness in accurately detecting pneumonia cases.
Together, these accuracy curves emphasize the model's consistent and remarkable performance across all datasets, achieving rapid convergence and near-perfect accuracy in each case.

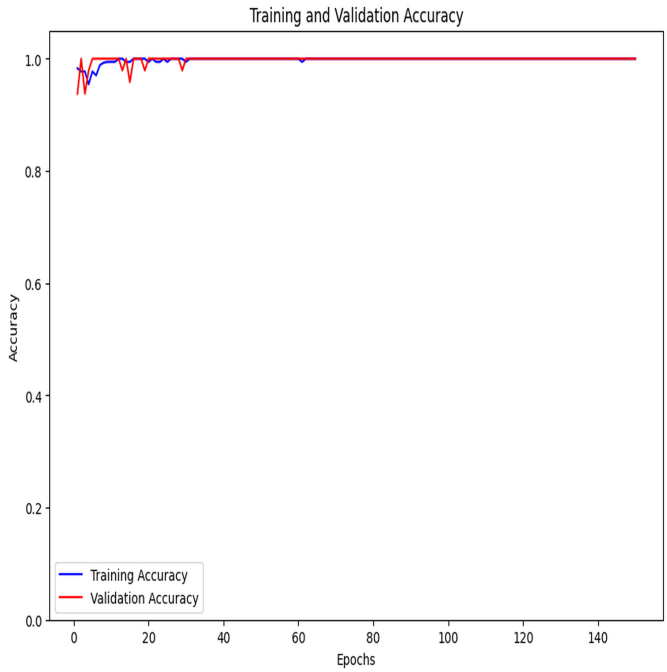

Fig. 6: Accuracy Curve of Brain Tumor

6.5 ROC Curves

ROC (Receiver Operating Characteristic) curves for the proposed CNN model involve using the model's predictions and true labels to calculate the true positive rate (sensitivity) and false positive rate at different classification thresholds. The model achieved AUC(Area under the ROC Curve) values of 1.0 for brain tumor, 1.0 for COVID-19, 0.94 for breast histopathology and 0.98 for pneumonia. From Fig. 10 to Fig.13, the curves illustrate the ROC curves of the proposed CNN model on the test datasets, where the x-axis represents the false positive rate and the y-axis represents the true positive rate.

6.6 Precision-Recall Curves

The precision-recall curves for the CNN model are generated by using the model's predictions and true labels to calculate precision and recall at different classification thresholds. From Fig. 14 to Fig.

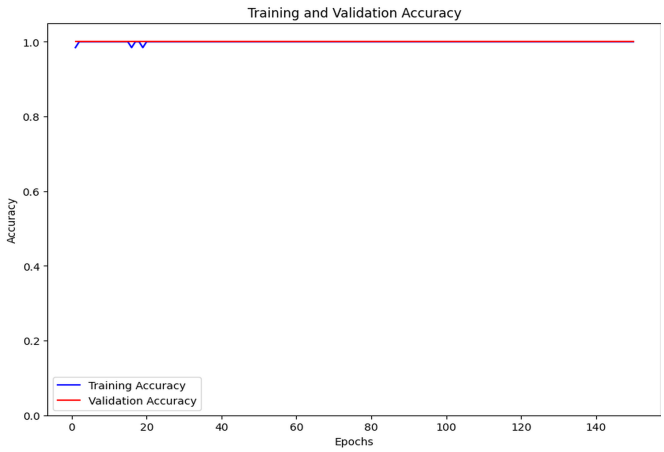

Fig. 7: Accuracy Curve of Covid19

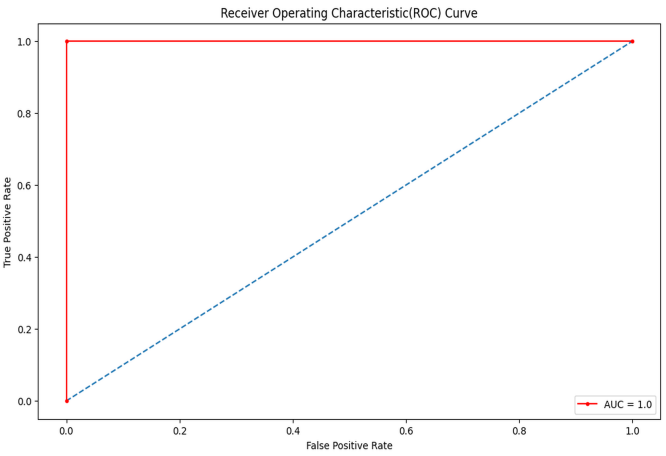

Fig. 10: ROC Curve of Brain Tumor

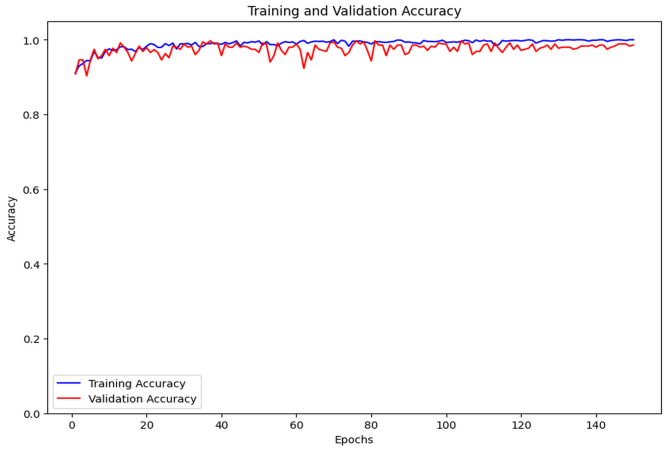

Fig. 8: Accuracy Curve of Breast Histopathology

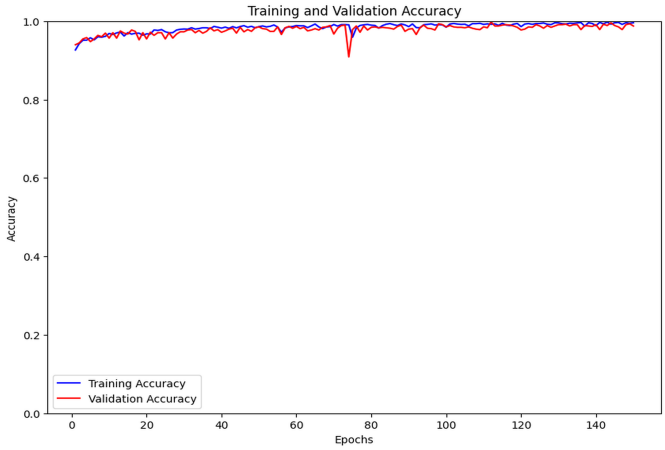

Fig. 9: Accuracy Curve of Pneumonia

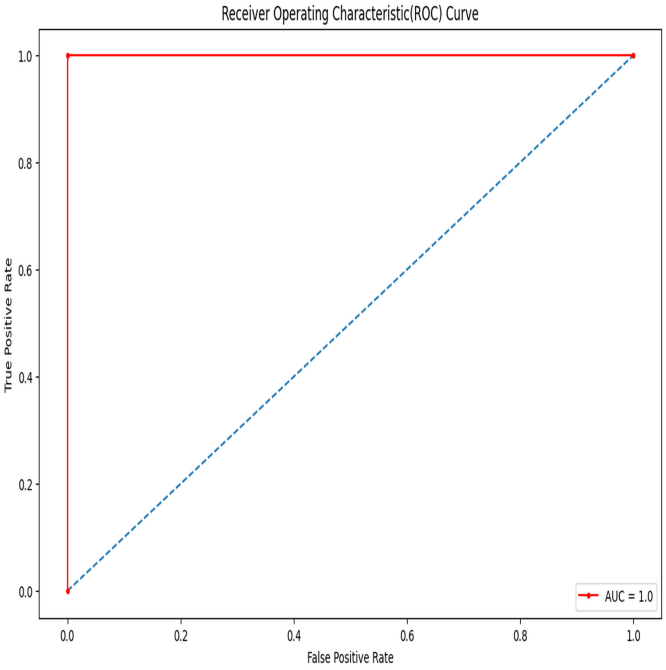

Fig. 11: ROC Curve of Covid-19

17, the curves illustrate the precision-recall performance of the proposed CNN model, where the x-axis represents recall and the y-axis represents precision on the test datasets.

6.7 Confusion Matrices

Figures 18 through 21 show the confusion matrices of the proposed CNN model on different category test datasets.

6.8 Test Dataset Output Images and Model Comparison:

In the test dataset, the data items are entirely unseen by the model and are used to evaluate its performance. Here, some results are

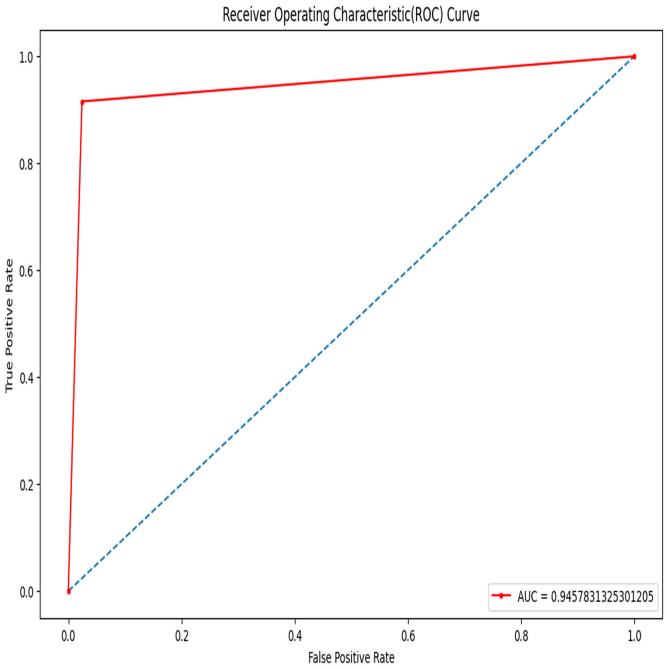

Fig. 12: ROC Curve of Breast Histopathology

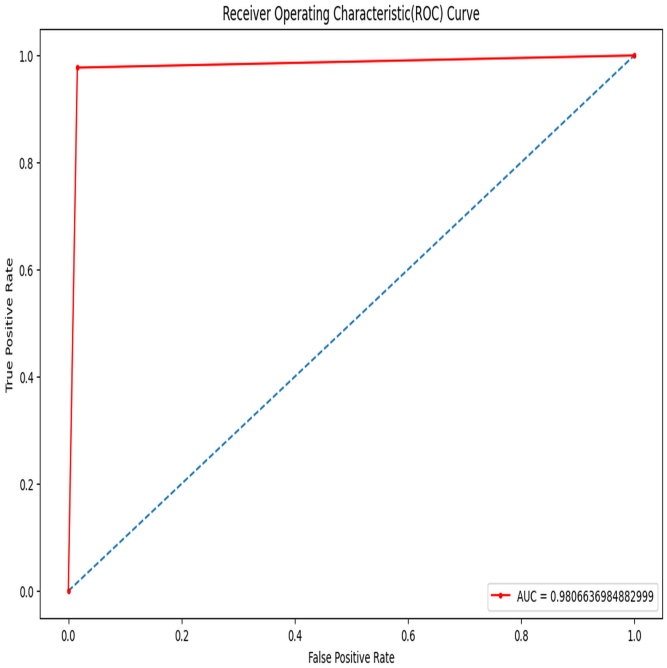

Fig. 13: ROC Curve of Pneumonia

presented in Fig. 22, Fig. 23, Fig. 24, Fig. 25 from the test datasets predicted by the model.

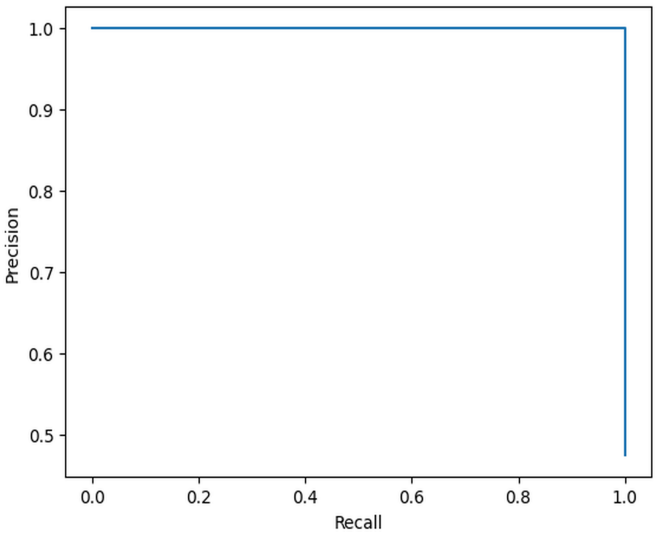

Fig. 14: Precision-Recall Curve of Brain Tumor

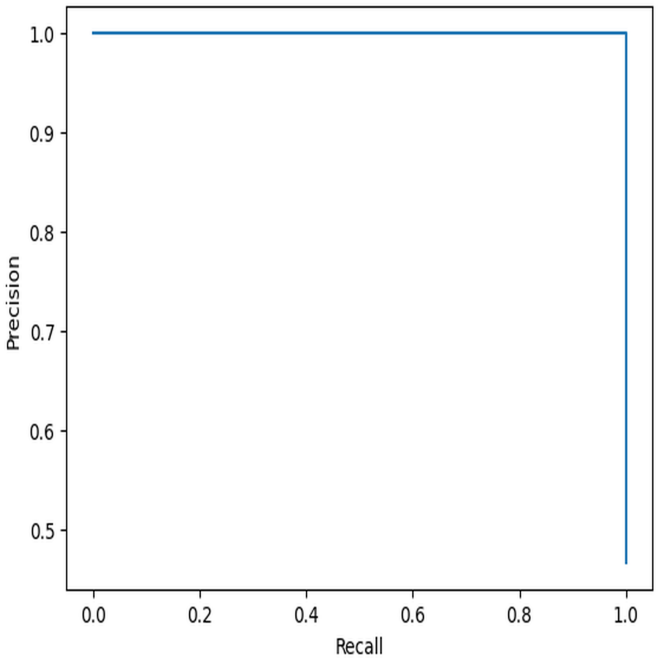

Fig. 15: Precision-Recall Curve of Covid-19

6.9 Ablation Study on Key Components of the Proposed Framework(Brain Tumor Dataset)

An ablation study was conducted to evaluate the contribution of individual components in the proposed framework using the Brain Tumor dataset. The baseline model was trained directly on imbalanced data without any resampling or pretraining. Introducing data augmentation resulted in noticeable performance improvements by reducing overfitting, while the inclusion of weighted random sampling further enhanced classification accuracy by effectively ad-

Table 2. : Comparison Table

Datasets	Models	Precision	Recall	Specificity	Accuracy	F1 Score	J-Score	MCC	FAR	FRR	EER
COVID-19	VGG16	1.0	0.43	1.0	0.7333	0.6	0.43	0.53	0	0.57	0.28
	VGG19	1.0	0.8571	1.0	0.9333	0.9230	0.8571	0.87	0	0.143	0.071
	Resnet152	1.0	0.7143	1.0	0.8666	0.8333	0.7143	0.756	0	0.29	0.143
	InceptionV3	1.0	0.43	1.0	0.7333	0.6	0.428	0.53	0	0.57	0.29
	Densenet121	1.0	0.428	1.0	0.73	0.6	0.428	0.53	0	0.57	0.286
	Proposed Model	**0.9998**	**0.9996**	**1.0**	**0.9996**	**0.9997**	**0.9996**	**0.9996**	**0**	**0.0004**	**0.0002**
Brain Tumor	VGG16	1.0	0.9565	1.0	0.975	0.977	0.9565	0.9504	0	0.043	0.022
	VGG19	1.0	0.95	1.0	0.975	0.9743	0.95	0.9511	0	0.05	0.025
	Resnet152	1.0	1.0	1.0	1.0	1.0	1.0	1.0	0	0	0
	InceptionV3	1.0	1.0	1.0	1.0	1.0	1.0	1.0	0	0	0
	Densenet121	1.0	0.9615	1.0	0.975	0.98	0.9615	0.9473	0	0.038	0.019
	Proposed Model	**0.9997**	**0.9997**	**1.0**	**0.9997**	**0.9997**	**0.9997**	**0.9997**	**0**	**0.0003**	**0.00015**
Breast Histopathology	VGG16	0.9737	0.6981	0.98	0.8396	0.8132	0.6792	0.7082	0.019	0.302	0.160
	VGG19	0.9722	0.66	0.98	0.8207	0.7865	0.6415	0.019	0	0.34	0.18
	Resnet152	1.0	0.87	1.0	0.9339	0.9292	0.8679	0.88	0	0.132	0.066
	InceptionV3	0.9729	0.68	0.98	0.8302	0.799	0.66	0.69	0.019	0.32	0.17
	Densenet121	0.9761	0.77	0.98	0.88	0.863	0.755	0.77	0.019	0.23	0.123
	Proposed Model	**0.9698**	**0.9277**	**0.9698**	**0.9487**	**0.9476**	**0.8975**	**0.8983**	**0.030**	**0.072**	**0.051**
Pneumonia	VGG16	0.9787	0.938	0.946	0.9408	0.9584	0.885	0.86	0.054	0.061	0.057
	VGG19	0.9695	0.9881	0.897	0.9670	0.9787	0.8852	0.9062	0.103	0.012	0.057
	Resnet152	0.9860	0.9606	0.959	0.9602	0.9731	0.9195	0.8974	0.041	0.039	0.040
	InceptionV3	0.9836	0.9836	0.9471	0.9749	0.9836	0.9307	0.9307	0.053	0.016	0.035
	Densenet121	0.98	0.98	0.946	0.9738	0.9833	0.9272	0.917	0.054	0.019	0.032
	Proposed Model	**0.9628**	**1.0**	**0.9613**	**0.9806**	**0.9810**	**0.9613**	**0.9620**	**0.039**	**0.0**	**0.019**

MCC:- Matthews correlation coefficient, FAR:- False Acceptance Rate, FRR:- False Rejection Rate, EER: Equal Error Rate.

N.B.: All evaluation metrics in this comparison table and the associated visual analyses, including AUC values, ROC curves, and confusion matrices, are computed using the test dataset, except for the loss and accuracy curves, which are generated from the training and validation datasets.

dressing class imbalance during training. Balanced dataset pretraining contributed to more stable and discriminative feature learning. The complete framework, integrating all components, achieved the highest performance, demonstrating that each module plays a com-

Table 3. : Ablation Study on Key Components of the Proposed Model

Configuration	Balanced Pretraining	Weighted Random Sampling	Data Augmentation	Test Accuracy (%)
Baseline CNN (direct training on imbalanced data)	✗	✗	✗	86.82
Data Augmentation	✗	✗	✓	90.94
Weighted Random Sampling	✗	✓	✓	96.71
Balanced Dataset Pretraining	✓	✗	✓	98.12
Proposed Model	✓	✓	✓	99.97

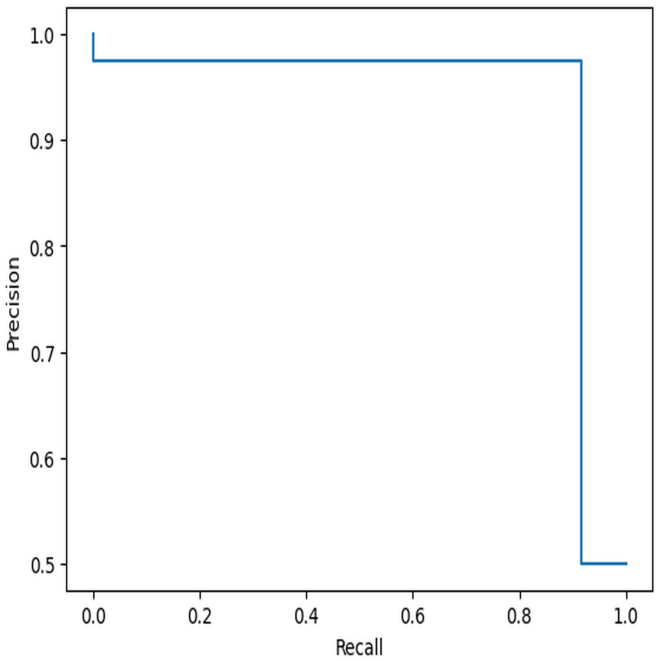

Fig. 16: Precision-Recall Curve of Breast Histopathology

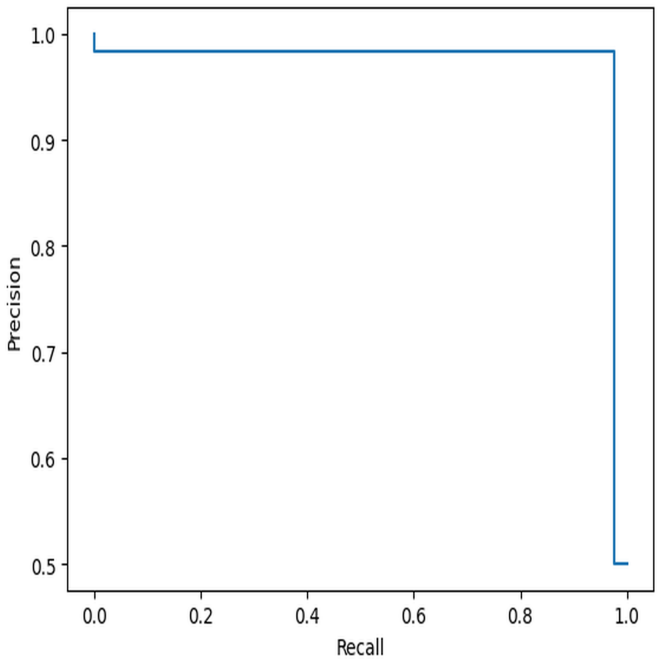

Fig. 17: Precision-Recall Curve of Pneumonia

plementary role in improving classification accuracy. Although the ablation study is reported in detail for the Brain Tumor dataset, similar performance trends were consistently observed for the COVID-19, Breast Histopathology, and Pneumonia datasets. In all cases, the inclusion of balanced pretraining, data augmentation, and weighted random sampling contributed positively to classification performance. For brevity and to avoid redundancy, detailed ablation results for these additional datasets are not presented.

7. APPENDICES

The datasets used in this study can be accessed through the following links:

—Brain Tumor Imbalanced Dataset
—Covid-19 Imbalanced Dataset
—Breast Histopathology Imbalanced Dataset
—Pneumonia Imbalanced Dataset
—Brain Tumor Balanced Dataset
—Covid-19 Balanced Dataset
—Breast Histopathology Balanced Dataset
—Pneumonia Balanced Dataset

8. CONCLUSION

The development and evaluation of a comprehensive Convolutional Neural Network (CNN)-based model for the simultaneous detection and classification of brain tumors, COVID-19 infections,breast histopathological anomalies, and pneumonia represent a significant advancement in the field of medical diagnostics. This research demonstrates the potential to enhance the accuracy, efficiency, and scalability of disease detection across diverse pathological conditions by integrating AI-driven approaches and multimodal medical imaging data.

The findings of this study underscore the effectiveness of the proposed CNN model in achieving high accuracy, sensitivity and

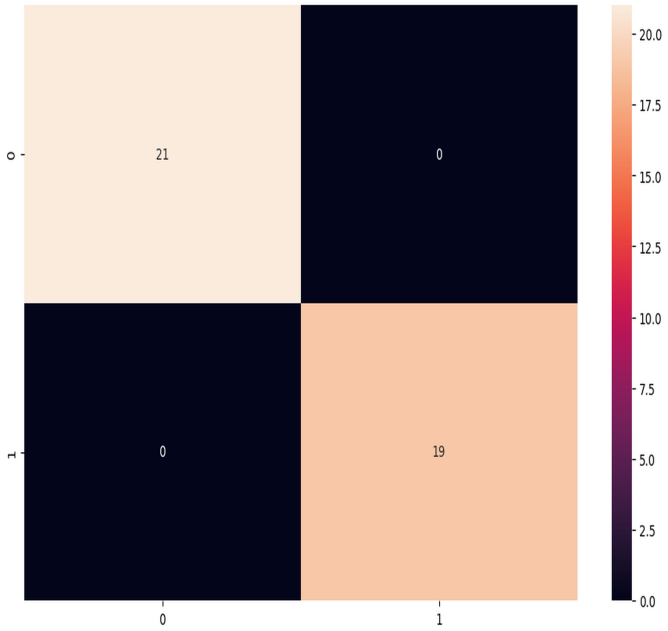

Fig. 18: Confusion Matrix of Brain Tumor

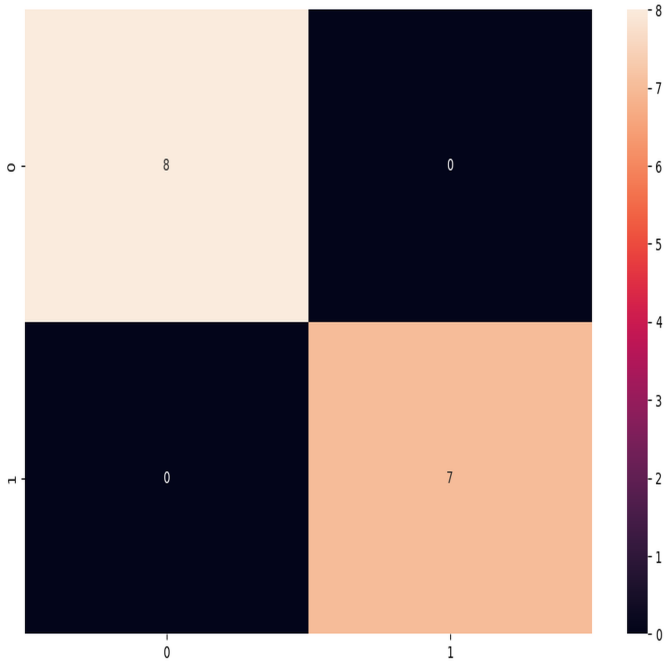

Fig. 19: Confusion Matrix of Covid-19

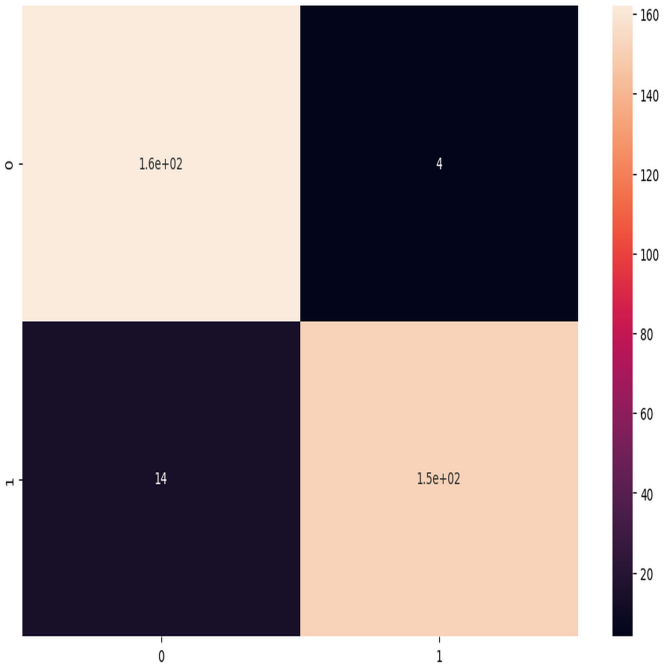

Fig. 20: Confusion Matrix of Breast Histopathology

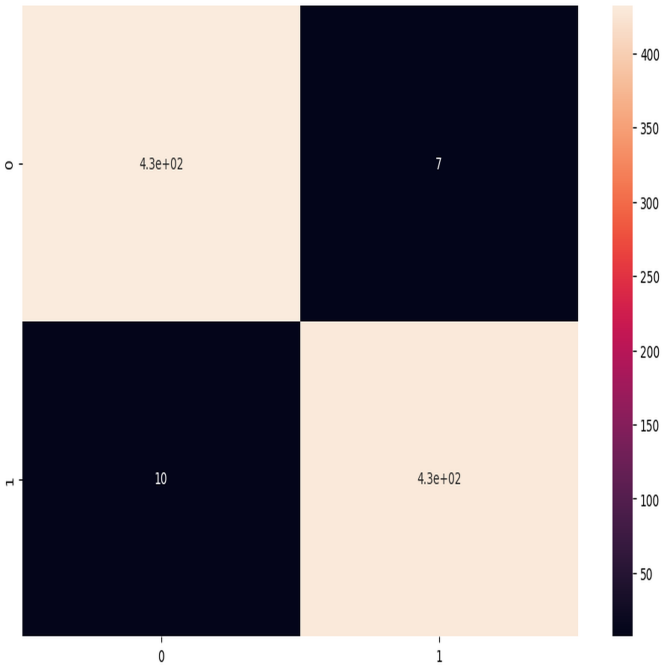

Fig. 21: Confusion Matrix of Pneumonia

specificity in disease detection and classification. By leveraging deep learning techniques and multimodal medical imaging data, the model has shown promising results in accurately identifying and distinguishing between different disease entities, thereby facilitating timely and precise diagnostic decision-making.

Furthermore, the development of a versatile CNN model capable of simultaneously detecting and classifying multiple diseases addresses critical gaps in current diagnostic approaches. The model's ability to analyze diverse medical imaging modalities, including MRI, CT, chest x-rays, and histopathological images, highlights its

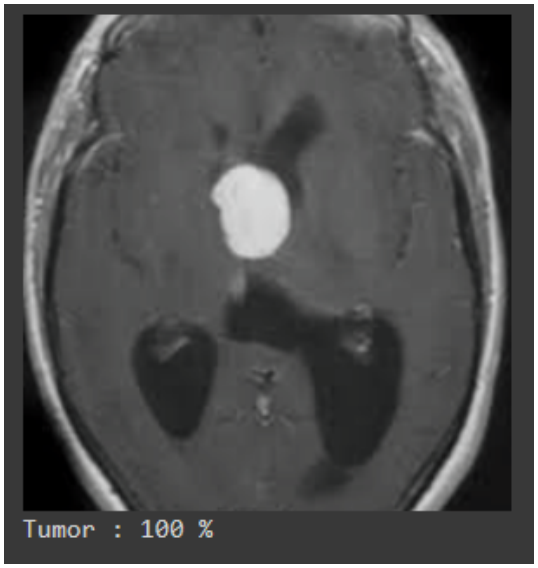

Fig. 22: brain tumor

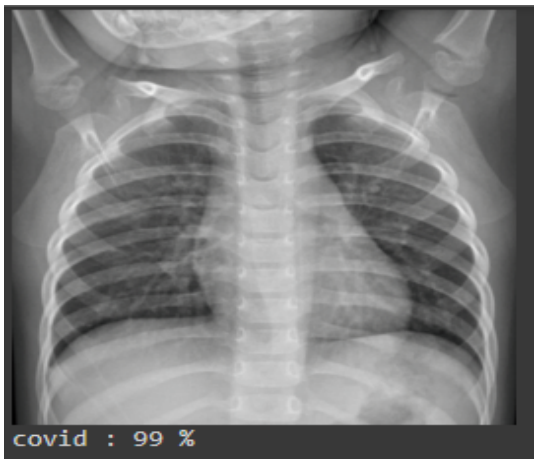

Fig. 23: covid-19

versatility and potential for widespread clinical application across various healthcare settings.

The implications of this research extend beyond the realm of disease detection and classification, offering opportunities to streamline clinical workflows, improve diagnostic accuracy, and ultimately enhance patient outcomes. By automating the process of disease diagnosis, the proposed CNN model has the potential to reduce the burden on healthcare practitioners, mitigate interobserver variability, and expedite treatment initiation, particularly in time-sensitive scenarios such as acute respiratory infections and cancer diagnosis.

However, it is essential to acknowledge the limitations of the proposed CNN model, including the need for further validation and refinement using larger, more diverse datasets. Additionally, the interpretability of the model's predictions and the integration of clinical context into diagnostic decision-making warrant further investigation to ensure the model's clinical utility and acceptance by healthcare practitioners.

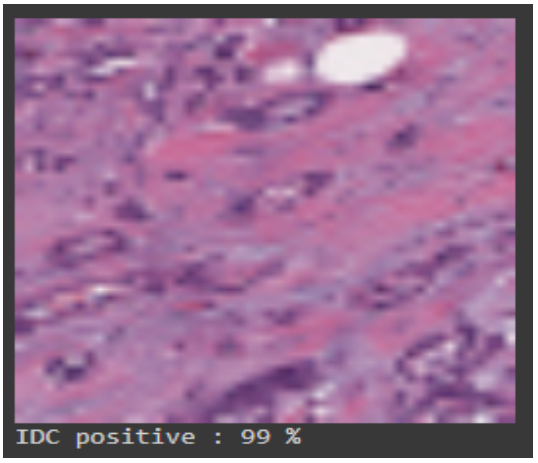

Fig. 24: breast histopathology

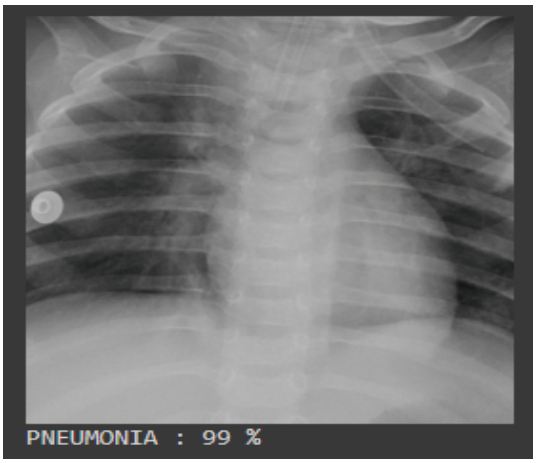

Fig. 25: pneumonia

Moving forward, future research directions may include the development of more sophisticated CNN architectures, the incorporation of additional clinical variables and biomarkers and the integration of real-time data streams for continuous disease monitoring and prediction. Furthermore, collaboration between interdisciplinary teams of clinicians, data scientists and AI researchers is crucial for translating AI-driven diagnostic tools from research prototypes to clinically deployable solutions.

The integration of quantum computing into CNN-based models may hold immense potential to further enhance the capabilities and performance of medical diagnostic systems. Quantum computing offers unparalleled computational power and the ability to process vast amounts of data in parallel, making it ideally suited for complex and computationally intensive tasks such as medical image analysis.

In conclusion, the proposed CNN model represents a significant step forward in advancing the field of AI-driven medical diagnostics, with the potential to revolutionize disease detection and classification across multiple pathological conditions. By harnessing the power of deep learning and multimodal medical imaging data, this research contributes to the ongoing efforts to improve healthcare outcomes and enhance patient care in the era of precision medicine.

9. REFERENCES

[1] Ahmed H Abdel-Gawad, Lobna A Said, and Ahmed G Radwan. Optimized edge detection technique for brain tumor detection in mr images. *IEEE Access*, 8:136243–136259, 2020.

[2] Nyoman Abiwinanda, Muhammad Hanif, S Tafwida Hesaputra, Astri Handayani, and Tati Rajab Mengko. Brain tumor classification using convolutional neural network. In *World Congress on Medical Physics and Biomedical Engineering 2018: June 3-8, 2018, Prague, Czech Republic (Vol. 1)*, pages 183–189. Springer, 2019.

[3] Parnian Afshar, Arash Mohammadi, and Konstantinos N Plataniotis. Brain tumor type classification via capsule networks. In *2018 25th IEEE international conference on image processing (ICIP)*, pages 3129–3133. IEEE, 2018.

[4] Hayat O Alasasfeh, Taqwa Alomari, and MS Ibbini. Deep learning approach for covid-19 detection based on x-ray images. In *2021 18th International Multi-Conference on Systems, Signals & Devices (SSD)*, pages 1–6. IEEE, 2021.

[5] Javeria Amin, Muhammad Sharif, Mussarat Yasmin, and Steven Lawrence Fernandes. Big data analysis for brain tumor detection: Deep convolutional neural networks. *Future Generation Computer Systems*, 87:290–297, 2018.

[6] Jun Cheng. Brain tumor dataset. *figshare. Dataset*, 1512427(5), 2017.

[7] Sreeparna Das, Ishan Ayus, and Deepak Gupta. A comprehensive review of covid-19 detection with machine learning and deep learning techniques. *Health and Technology*, pages 1–14, 2023.

[8] Mohammad Havaei, Axel Davy, David Warde-Farley, Antoine Biard, Aaron Courville, Yoshua Bengio, Chris Pal, Pierre-Marc Jodoin, and Hugo Larochelle. Brain tumor segmentation with deep neural networks. *Medical image analysis*, 35:18–31, 2017.

[9] Shrutika Santosh Hunnur, Akshata Raut, and Swati Kulkarni. Implementation of image processing for detection of brain tumors. In *2017 International Conference on Computing Methodologies and Communication (ICCMC)*, pages 717–722. IEEE, 2017.

[10] Yohan Jun, Taejoon Eo, Taeseong Kim, Hyungseob Shin, Dosik Hwang, So Hi Bae, Yae Won Park, Ho-Joon Lee, Byoung Wook Choi, and Sung Soo Ahn. Deep-learned 3d black-blood imaging using automatic labelling technique and 3d convolutional neural networks for detecting metastatic brain tumors. *Scientific reports*, 8(1):9450, 2018.

[11] Naresh Khuriwal and Nidhi Mishra. Breast cancer detection from histopathological images using deep learning. In *2018 3rd international conference and workshops on recent advances and innovations in engineering (ICRAIE)*, pages 1–4. IEEE, 2018.

[12] Gulshan Kumar, Puneet Kumar, and Deepika Kumar. Brain tumor detection using convolutional neural network. In *2021 IEEE International Conference on Mobile Networks and Wireless Communications (ICMNWC)*, pages 1–6. IEEE, 2021.

[13] Tingting Liu, Zhi Yuan, Li Wu, and Benjamin Badami. An optimal brain tumor detection by convolutional neural network and enhanced sparrow search algorithm. *Proceedings of the Institution of Mechanical Engineers, Part H: Journal of Engineering in Medicine*, 235(4):459–469, 2021.

[14] Shraddha S More, Mansi Ashok Mange, Mitheel Sandip Sankhe, and Shwethali Santosh Sahu. Convolutional neural network based brain tumor detection. In *2021 5th International conference on intelligent computing and control systems (ICICCS)*, pages 1532–1538. IEEE, 2021.

[15] Ayush Pant, Akshat Jain, Kiran C Nayak, Daksh Gandhi, and BG Prasad. Pneumonia detection: An efficient approach using deep learning. In *2020 11th International Conference on Computing, Communication and Networking Technologies (ICCCNT)*, pages 1–6. IEEE, 2020.

[16] J Seetha and S Selvakumar Raja. Brain tumor classification using convolutional neural networks. *Biomedical & Pharmacology Journal*, 11(3):1457, 2018.

[17] Ghada A Shadeed, Abdullah A Jabber, and Nahedh H Alwash. I. covid-19 detection using deep learning models. In *2021 1st Babylon international conference on information technology and science (BICITS)*, pages 194–198. IEEE, 2021.

[18] Komal Sharma, Akwinder Kaur, and Shruti Gujral. Brain tumor detection based on machine learning algorithms. *International Journal of Computer Applications*, 103(1), 2014.

[19] Swapnil Singh. Pneumonia detection using deep learning. In *2021 4th Biennial International Conference on Nascent Technologies in Engineering (ICNTE)*, pages 1–6. IEEE, 2021.

[20] Fabio Alexandre Spanhol, Luiz S Oliveira, Caroline Petitjean, and Laurent Heutte. Breast cancer histopathological image classification using convolutional neural networks. In *2016 international joint conference on neural networks (IJCNN)*, pages 2560–2567. IEEE, 2016.